

# A high C/O ratio and weak thermal inversion in the atmosphere of exoplanet WASP-12b

Nikku Madhusudhan<sup>1†</sup>, Joseph Harrington<sup>2</sup>, Kevin B. Stevenson<sup>2</sup>, Sarah Nymeyer<sup>2</sup>, Christopher J. Campo<sup>2</sup>, Peter J. Wheatley<sup>3</sup>, Drake Deming<sup>4</sup>, Jasmina Blecic<sup>2</sup>, Ryan A. Hardy<sup>2</sup>, Nate B. Lust<sup>2</sup>, David R. Anderson<sup>5</sup>, Andrew Collier-Cameron<sup>6</sup>, Christopher B. T. Britt<sup>2</sup>, William C. Bowman<sup>2</sup>, Leslie Hebb<sup>7</sup>, Coel Hellier<sup>5</sup>, Pierre F. L. Maxted<sup>5</sup>, Don Pollacco<sup>8</sup> & Richard G. West<sup>9</sup>

The carbon-to-oxygen ratio (C/O) in a planet provides critical information about its primordial origins and subsequent evolution. A primordial C/O greater than 0.8 causes a carbide-dominated interior, as opposed to the silicate-dominated composition found on Earth<sup>1</sup>; the atmosphere can also differ from those in the Solar System<sup>1,2</sup>. The solar C/O is 0.54 (ref. 3). Here we report an analysis of dayside multi-wavelength photometry<sup>4,5</sup> of the transiting hot-Jupiter WASP-12b (ref. 6) that reveals  $C/O \geq 1$  in its atmosphere. The atmosphere is abundant in CO. It is depleted in water vapour and enhanced in methane, each by more than two orders of magnitude compared to a solar-abundance chemical-equilibrium model at the expected temperatures. We also find that the extremely irradiated atmosphere ( $T > 2,500$  K) of WASP-12b lacks a prominent thermal inversion (or stratosphere) and has very efficient day-night energy circulation. The absence of a strong thermal inversion is in stark contrast to theoretical predictions for the most highly irradiated hot-Jupiter atmospheres<sup>7-9</sup>.

The transiting hot Jupiter WASP-12b orbits a star slightly hotter than the Sun (6,300 K) in a circular orbit at a distance of only 0.023 astronomical units (AU), making it one of the hottest exoplanets known<sup>6</sup>. Thermal emission from the dayside atmosphere of WASP-12b has been reported using the Spitzer Space Telescope<sup>10</sup>, at 3.6  $\mu\text{m}$ , 4.5  $\mu\text{m}$ , 5.8  $\mu\text{m}$  and 8  $\mu\text{m}$  wavelengths<sup>4</sup>, and from ground-based observations in the J (1.2  $\mu\text{m}$ ), H (1.6  $\mu\text{m}$ ) and Ks (2.1  $\mu\text{m}$ ) bands<sup>5</sup> (Fig. 1).

The observations provide constraints on the dayside atmospheric composition and thermal structure, based on the dominant opacity source in each bandpass. The J, H and Ks channels<sup>5</sup> have limited molecular absorption features, and hence probe the deep layers of the planetary atmosphere, at pressure  $P \approx 1$  bar, where the temperature  $T \approx 3,000$  K (Fig. 1). The Spitzer observations<sup>4</sup>, on the other hand, are excellent probes of molecular composition. CH<sub>4</sub> has strong absorption features in the 3.6- $\mu\text{m}$  and 8- $\mu\text{m}$  channels, CO has strong absorption in the 4.5- $\mu\text{m}$  channel, and H<sub>2</sub>O has its strongest feature in the 5.8- $\mu\text{m}$  channel and weaker features in the 3.6- $\mu\text{m}$ , 4.5- $\mu\text{m}$  and 8- $\mu\text{m}$  channels. The low brightness temperatures in the 3.6- $\mu\text{m}$  (2,700 K) and 4.5- $\mu\text{m}$  (2,500 K) channels, therefore, clearly suggest strong absorption due to CH<sub>4</sub> and CO, respectively. The high brightness temperature in the 5.8- $\mu\text{m}$  channel, on the other hand, indicates low absorption due to H<sub>2</sub>O. The strong CO absorption in the 4.5- $\mu\text{m}$  channel also indicates temperature decreasing with altitude, because a thermal inversion would cause emission features of CO in the same channel with a significantly higher flux than at 3.6  $\mu\text{m}$  (refs 11 and 12).

The broadband observations allow us to infer the chemical composition and temperature structure of the dayside atmosphere of WASP-12b using a statistical retrieval technique<sup>11</sup>. We combined a one-dimensional atmosphere model with a Markov-chain Monte Carlo sampler<sup>11,13</sup> that computes over  $4 \times 10^6$  models to explore the

parameter space. The phase space included thermal profiles with and without inversions, and equilibrium and non-equilibrium chemistry over a wide range of atomic abundances. Our models include the dominant sources of infrared opacity in the temperature regime of WASP-12b (refs 14, 15 and 16): H<sub>2</sub>O, CO, CH<sub>4</sub>, CO<sub>2</sub>, H<sub>2</sub>-H<sub>2</sub> collision-induced absorption, and TiO and VO where the temperatures

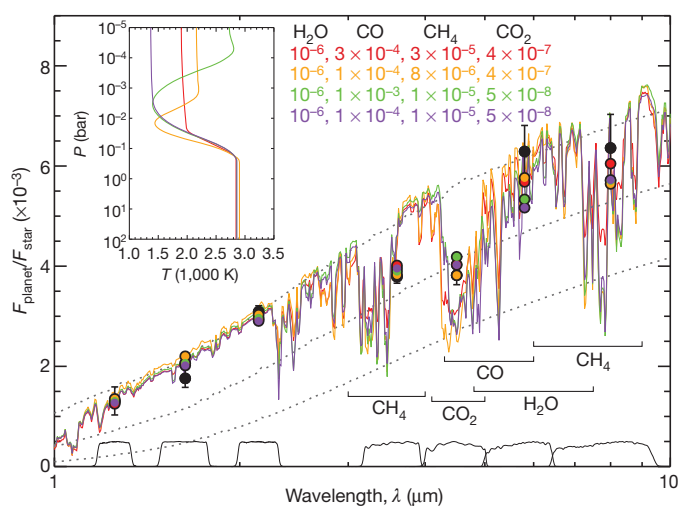


**Figure 1 | Observations and model spectra for dayside thermal emission of WASP-12b.**  $F$  is the flux. The black filled circles with error bars show the data with 1 s.d. errors: four Spitzer observations<sup>4</sup> (3.6  $\mu\text{m}$ , 4.5  $\mu\text{m}$ , 5.8  $\mu\text{m}$  and 8  $\mu\text{m}$ ), and three ground-based observations in the J (1.2  $\mu\text{m}$ ), H (1.6  $\mu\text{m}$ ), and Ks (2.1  $\mu\text{m}$ ) bands<sup>5</sup>. Four models fitting the observations are shown in the coloured solid curves in the main panel, and the coloured circles are the channel-integrated model points. The corresponding temperature profiles are shown in the inset. The molecular compositions are shown as number ratio with respect to molecular hydrogen; all the models have C/O between 1 and 1.1. The thin grey dotted lines show the blackbody spectra of WASP-12b at 2,000 K (bottom), 2,500 K (middle) and 3,000 K (top). A Kurucz model<sup>29</sup> was used for the stellar spectrum, assuming uniform illumination over the planetary disk (that is, weighted by 0.5; ref. 7). The black solid lines at the bottom show the photometric band-passes in arbitrary units. The low fluxes at 3.6  $\mu\text{m}$  and 4.5  $\mu\text{m}$  are explained by methane and CO absorption, respectively, required for all the models that fit. The high flux in the 5.8- $\mu\text{m}$  channel indicates less absorption due to H<sub>2</sub>O. The observations can be explained to high precision by models without thermal inversions. Models with strong thermal inversions are ruled out by the data (see Fig. 3). The green model features a thermal inversion at low pressures ( $P < 0.01$  bar), but the corresponding spectrum is almost indistinguishable from the purple model, which does not have a thermal inversion; both models have identical compositions and identical thermal profiles for  $P > 0.01$  bar. Thus, any potential thermal inversion is too weak to be detectable by current instruments.

<sup>1</sup>Massachusetts Institute of Technology, Cambridge, Massachusetts 02139, USA. <sup>2</sup>Planetary Sciences Group, Department of Physics, University of Central Florida, Orlando, Florida 32816-2385, USA. <sup>3</sup>Department of Physics, University of Warwick, Coventry, CV4 7AL, UK. <sup>4</sup>NASA's Goddard Space Flight Center, Greenbelt, Maryland 20771-0001, USA. <sup>5</sup>Astrophysics Group, Keele University, Staffordshire ST5 5BG, UK. <sup>6</sup>School of Physics and Astronomy, University of St Andrews, North Haugh, Fife KY16 9SS, UK. <sup>7</sup>Department of Physics and Astronomy, Vanderbilt University, Nashville, Tennessee 37235, USA. <sup>8</sup>Astrophysics Research Centre, School of Mathematics and Physics, Queen's University, University Road, Belfast, BT7 1NN, UK. <sup>9</sup>Department of Physics and Astronomy, University of Leicester, Leicester, LE1 7RH, UK. <sup>†</sup>Present address: Department of Astrophysical Sciences, Princeton University, Princeton, New Jersey 08544, USA.

are high enough for them to exist in the gas phase<sup>7,17</sup>. The host star has a significantly enhanced metallicity ( $2 \times$  solar)<sup>6</sup>, and evolutionary processes can further enhance the abundances<sup>18,19</sup>; Jupiter has  $3 \times$  solar C/H (ref. 18). Our models therefore explore wide abundance ranges:  $0.01\text{--}100 \times$  solar for C/H and O/H, and  $0.1\text{--}10 \times$  solar for C/O. Figure 2 shows the mixing ratios of H<sub>2</sub>O, CO, CH<sub>4</sub> and CO<sub>2</sub> and the ratios of C/H, O/H and C/O required by the models at different levels of fit. Figure 3 presents the temperature profiles.

We find a surprising lack of water and overabundance of methane (Fig. 2). At 2,000–3,000 K, assuming solar abundances yields CO and H<sub>2</sub>O as the dominant species besides H<sub>2</sub> and He (refs 15 and 16). Most of the carbon, and the same amount of oxygen, are present in CO, and some carbon exists as CH<sub>4</sub>. The remaining oxygen in a hydrogen-dominated atmosphere is mostly in H<sub>2</sub>O; small amounts are also present in species such as CO<sub>2</sub>. The CO/H<sub>2</sub> and H<sub>2</sub>O/H<sub>2</sub> mixing ratios should each be  $>5 \times 10^{-4}$ , CH<sub>4</sub>/H<sub>2</sub> should be  $<10^{-8}$ , and CO<sub>2</sub>/H<sub>2</sub> should be about  $10^{-8}$ , under equilibrium conditions at a nominal pressure of 0.1 bar. The requirement of H<sub>2</sub>O/H<sub>2</sub>  $\leq 6 \times 10^{-6}$  and CH<sub>4</sub>/H<sub>2</sub>  $\geq 8 \times 10^{-6}$  (both at  $3\sigma$ , 99.73% significance; Fig. 2) is therefore inconsistent with equilibrium chemistry using solar abundances.

The observations place a strict constraint on the C/O ratio. We detect C/O  $\geq 1$  at  $3\sigma$  significance (Fig. 2). Our results rule out a solar C/O of 0.54 at  $4.2\sigma$ . Our calculations of equilibrium chemistry<sup>16,20</sup> using C/O = 1 yield mixing ratios of H<sub>2</sub>O, CO and CH<sub>4</sub> that are consistent with the observed constraints. We find that, for C/O = 1, H<sub>2</sub>O mixing ratios as low as  $10^{-7}$  and CH<sub>4</sub> mixing ratios as high as  $10^{-5}$  can be attained at the 0.1–1 bar level for temperatures around 2,000 K and higher. And, although the CO mixing ratio is predicted to be  $>10^{-4}$ , making it the dominant molecule after H<sub>2</sub> and He, CO<sub>2</sub> is predicted to be negligible ( $<10^{-9}$ ). The theoretical predictions for a

C/O = 1 atmosphere are consistent with the observed constraints on H<sub>2</sub>O, CH<sub>4</sub>, CO and CO<sub>2</sub> (Fig. 2).

The observations rule out a strong thermal inversion deeper than 0.01 bar (Fig. 3). Thermal inversions at lower pressures have opacities too low to induce features in the emission spectrum that current instruments can resolve. For comparison<sup>11,12,21</sup>, all stratospheric inversions in Solar System giant planets, and those consistent with hot-Jupiter observations, exist at pressures between 0.01 bar and 1 bar. The major contributions to all the observations come from the lower layers of the atmosphere,  $P > 0.01$  bar, where we rule out a thermal inversion (Supplementary Fig. 1). The observations also suggest very efficient day–night energy redistribution (Fig. 2). The low brightness temperatures at 3.6  $\mu\text{m}$  and 4.5  $\mu\text{m}$  imply that only part of the incident stellar energy is re-radiated from the dayside, whereas up to 45% is absorbed and redistributed to the nightside. The possibility of a deep thermal inversion and inefficient redistribution was suggested recently<sup>5</sup>, based on observations in the J, H and Ks channels, but the Spitzer observations rule out both conditions.

The lack of a prominent thermal inversion contrasts with recent work that designates WASP-12b as a member of the class of very hot Jupiters that are expected to host inversions<sup>7,22</sup>. At  $T > 2,000$  K, molecules such as TiO and VO, which are strong absorbers in the ultraviolet/visible, are expected to be in gas phase and potentially cause thermal inversions<sup>7</sup>. WASP-12b, now being the hottest planet without a distinct inversion, presents a major challenge to existing atmospheric classification schemes for exoplanets based on thermal inversions<sup>7,22</sup>. Although there are hints of low chromospheric activity<sup>8</sup> in the host star, it remains to be seen whether the high incident continuum ultraviolet flux expected for WASP-12b might be efficient in photo-dissociating inversion-causing compounds, thus explaining the lack of a strong

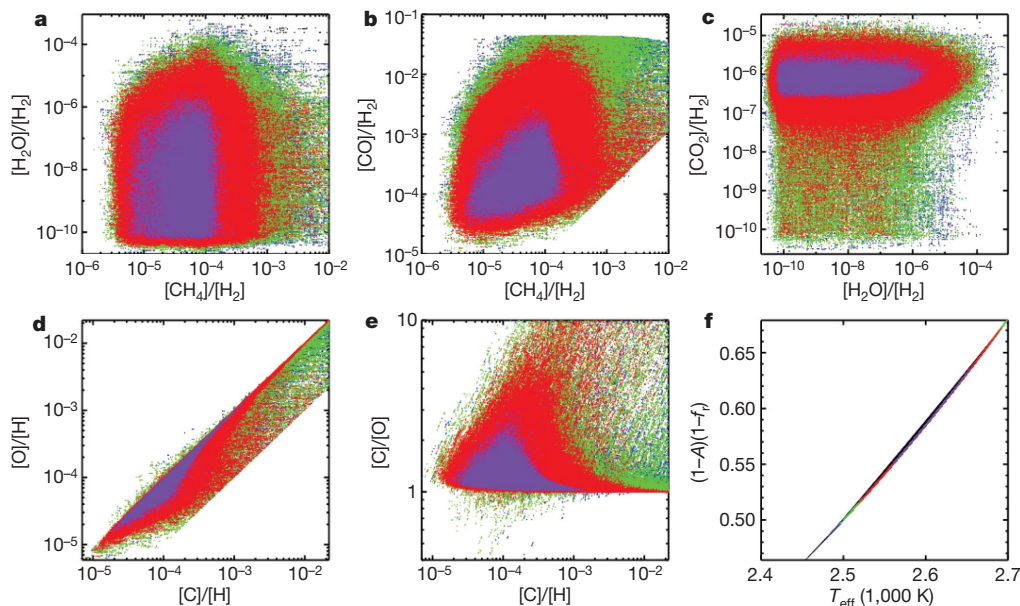


**Figure 2 | Constraints on the atmospheric composition of WASP-12b.**

**a–e** The distributions of models fitting the seven observations (Fig. 1) at different levels of  $\chi^2$  are shown. The coloured dots show  $\chi^2$  surfaces, with each dot representing a model realization. The purple, red, green, blue and black colours correspond to models with  $\chi^2$  less than 7, 14, 21 and 28 and  $\chi^2 > 28$ , respectively ( $\chi^2$  ranges between 4.8–51.3). Mixing ratios are shown as ratios by number with respect to H<sub>2</sub>. At  $3\sigma$  significance, the constraints on the composition are H<sub>2</sub>O/H<sub>2</sub>  $\leq 6 \times 10^{-6}$ , CH<sub>4</sub>/H<sub>2</sub>  $\geq 8 \times 10^{-6}$ , CO/H<sub>2</sub>  $\geq 6 \times 10^{-5}$ , CO<sub>2</sub>/H<sub>2</sub>  $\leq 5 \times 10^{-6}$ , and C/O  $> 1$ . The compositions of the best-fitting models (with  $\chi^2 < 7$ ) span H<sub>2</sub>O/H<sub>2</sub> =  $5 \times 10^{-11}$  to  $6 \times 10^{-6}$ , CO/H<sub>2</sub> =  $3 \times 10^{-5}$  to  $3 \times 10^{-3}$ , CH<sub>4</sub>/H<sub>2</sub> =  $4 \times 10^{-6}$  to  $8 \times 10^{-4}$  and CO<sub>2</sub>/H<sub>2</sub> =  $2 \times 10^{-7}$  to  $7 \times 10^{-6}$ ; the corresponding ranges in C/O and elemental abundances are C/O = 1 to 6.6, C/H =  $2 \times 10^{-5}$  to  $10^{-3}$  and O/H =  $2 \times 10^{-5}$

to  $10^{-3}$ . The constraints on the C/H and O/H ratios are governed primarily by the constraints on CO, which is the dominant molecule after H<sub>2</sub> and He. On the basis of thermochemical equilibrium, the inferred CH<sub>4</sub>/H<sub>2</sub> and H<sub>2</sub>O/H<sub>2</sub> mixing ratios are possible only for C/O  $\geq 1$ , consistent with our detection of C/O  $\geq 1$ . **f**, Constraints on the day–night energy redistribution<sup>11</sup>, given by  $(1-A)(1-f_r)$ , where  $A$  is the bond albedo and  $f_r$  is the fraction of incident energy redistributed to the nightside. Up to  $f_r = 0.45$  is possible (for  $A = 0$ ). Thus, the observations support very efficient redistribution. An additional observation in the z' (0.9  $\mu\text{m}$ ) band was reported recently<sup>30</sup>. However, the observation implies a value for the orbital eccentricity inconsistent with other data in the literature<sup>45</sup>. We therefore decided to exclude this observation from the analysis presented here, although including it does not affect our conclusions regarding the value of C/O or the temperature structure.

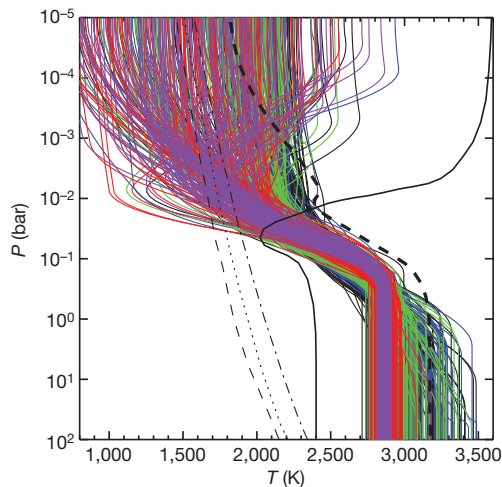


**Figure 3 | Thermal profiles of WASP-12b.** The solid thin lines show profiles at different degrees of fit (description of colours is as in Fig. 2); only 100 randomly chosen profiles for each  $\chi^2$  level are shown, for clarity. The thick black solid curve in the front shows a published profile from a self-consistent model of WASP-12b with a thermal inversion, adapted from ref. 17, which assumes solar abundances. The thick black dashed curve shows the same model but without a thermal inversion. If a thermal inversion is present in WASP-12b, it is expected to be prominent, as shown by the thick solid black curve. A prominent thermal inversion between 0.01 bar and 1 bar is ruled out by the data at  $4\sigma$ . The ostensibly large inversions in the figure are at low pressures (below 0.01 bar), which have low optical depths, and hence minimal influence on the emergent spectrum (see Fig. 1). The observations are completely consistent with thermal profiles having no inversions. Small thermal inversions are also admissible by the data, and could potentially result from dynamics. The thin black lines show the condensation curves of TiO at solar (dotted),  $0.1 \times$  solar (dashed) and  $10 \times$  solar (dash-dotted) compositions<sup>17</sup>.

inversion<sup>8</sup>. Alternatively, the amount of vertical mixing might be insufficient to keep TiO/VO aloft in the atmosphere to cause thermal inversions<sup>17</sup>. A C/O = 1 might also yield lower TiO/VO than that required to cause a thermal inversion. It is unlikely that the TiO/VO in WASP-12b might be lost to cold traps<sup>17</sup>, given the high temperatures in the deep atmosphere on the dayside and nightside.

If high C/O ratios are common, then the formation processes and compositions of extrasolar planets are probably very different from expectations based on Solar System planets. The host star has super-solar metallicity but initial analyses find its C/O consistent with solar<sup>6,23</sup>. In the core accretion model, favoured for the formation of Jupiter, icy planetesimals containing heavy elements coalesce to form the core, followed by gas accretion<sup>19,24</sup>. The abundances of elemental oxygen and carbon are enhanced equally<sup>18,19</sup>, maintaining a C/O like the star's. If the host star had a C/O  $\approx 1$ , then the C/O we detect in WASP-12b would have been evident. However, if the stellar C/O is indeed  $< 1$ , then the C/O enhancement in WASP-12b's atmosphere would suggest either an unexpected origin for the planetesimals, a local overdensity of carbonaceous grains<sup>2,25</sup>, or a different formation mechanism entirely. Although carbon-rich giant planets like WASP-12b have not been observed, theory predicts myriad compositions for carbon-dominated solid planets<sup>1,2</sup>. Terrestrial-sized carbon planets, for instance, could be dominated by graphite or diamond interiors, as opposed to the silicate composition of Earth<sup>1,2</sup>. If carbon dominates the heavy elements in the interior of a hot Jupiter, estimates of mass and radius could change compared to those based on solar abundances. Future interior models<sup>26</sup> should investigate the contribution of high C/O to the large radius of WASP-12b: that is, 1.75 Jupiter radii for 1.4 Jupiter masses (ref. 6).

The observed molecular abundances in the dayside atmosphere of WASP-12b motivate the exploration of a new regime in atmospheric chemistry. It remains to be seen whether photochemistry in WASP-12b

can significantly alter the composition in the lower layers of the atmosphere at  $P = 0.01$ –1 bar; these layers contribute most to the observed spectrum (Supplementary Fig. 1). Explaining the observed composition as a result of photochemistry with solar abundances would be challenging. CH<sub>4</sub> is more readily photodissociated than H<sub>2</sub>O (refs 9 and 27), and hence a depletion of CH<sub>4</sub> over that predicted with solar abundances might be expected, as opposed to the observed enhancement of CH<sub>4</sub>. Apart from the spectroscopically dominant molecules considered in this work, minor species such as OH, C<sub>2</sub>H<sub>2</sub> and FeH (refs 27 and 28), which are not detectable by current observations, could potentially be measured with high-resolution spectroscopy in the future. Detection of these species would allow additional constraints on equilibrium and non-equilibrium chemistry in WASP-12b, although their effect on the C/O would be negligible. Models of exoplanetary atmospheres have typically assumed solar abundances and/or solar C/O, thereby exploring a very limited region of parameter space<sup>7,12,20</sup>. Data sufficient for a meaningful constraint on C/O exist for only a few exoplanets. That this initial C/O statistical analysis has C/O  $\geq 1$  potentially indicates a wide diversity of planetary compositions.

Received 8 July; accepted 21 October 2010.

Published online 8 December 2010.

- Bond, J. C., O'Brien, D. P. & Lauretta, D. S. The compositional diversity of extrasolar planets. I. *In situ* simulations. *Astrophys. J.* **715**, 1050–1070 (2010).
- Kuchner, M. & Seager, S. Extrasolar carbon planets. Preprint at (<http://arxiv.org/abs/astro-ph/0504214>) (2005).
- Asplund, M., Grevesse, N. & Sauval, A. in *Cosmic Abundances as Records of Stellar Evolution and Nucleosynthesis* (eds Barnes, T. G. III & Bash, F. N.) 25–38 (ASP Conf. Ser. 336, 2005).
- Campo, C. *et al.* On the orbit of exoplanet WASP-12b. *Astrophys. J.* (in the press). Preprint at (<http://arxiv.org/abs/1003.2763>) (2010).
- Croll, B. *et al.* Near-infrared thermal emission from WASP-12b: detections of the secondary eclipse in Ks, H & J. *Astrophys. J.* (in the press). Preprint at (<http://arxiv.org/abs/1009.0071>) (2010).
- Hebb, L. *et al.* 2009, WASP-12b: the hottest transiting extrasolar planet yet discovered. *Astrophys. J.* **693**, 1920–1928 (2009).
- Fortney, J. J., Lodders, K., Marley, M. S. & Freedman, R. S. A unified theory for the atmospheres of the hot and very hot Jupiters: two classes of irradiated atmospheres. *Astrophys. J.* **678**, 1419–1435 (2008).
- Knutson, H. A., Howard, A. W. & Isaacson, H. A correlation between stellar activity and hot Jupiter emission spectra. *Astrophys. J.* **720**, 1569–1576 (2010).
- Zahnle, K. *et al.* Atmospheric sulfur photochemistry on hot Jupiters. *Astrophys. J.* **701**, L20–L24 (2009).
- Werner, M. W. *et al.* The Spitzer Space Telescope mission. *Astrophys. J. Suppl. Ser.* **154**, 1–9 (2004).
- Madhusudhan, N. & Seager, S. A temperature and abundance retrieval method for exoplanet atmospheres. *Astrophys. J.* **707**, 24–39 (2009).
- Burrows, A., Budaj, J. & Hubeny, I. Theoretical spectra and light curves of close-in extrasolar giant planets and comparison with data. *Astrophys. J.* **678**, 1436–1457 (2008).
- Gilks, W. R., Richardson, S. & Spiegelhalter, D. J. (eds) *Markov Chain Monte Carlo in Practice* (Chapman & Hall, 1996).
- Swain, M. R. *et al.* Molecular signatures in the near-infrared dayside spectrum of HD 189733b. *Astrophys. J.* **690**, L114–L117 (2009).
- Lodders, K. & Fegley, B. Atmospheric chemistry in giant planets, brown dwarfs, and low-mass dwarf stars. I. Carbon, nitrogen, and oxygen. *Icarus* **155**, 393–424 (2002).
- Burrows, A. & Sharp, C. M. Chemical equilibrium abundances in brown dwarf and extrasolar giant planet atmospheres. *Astrophys. J.* **512**, 843–863 (1999).
- Spiegel, D. S., Silverio, K. & Burrows, A. Can TiO explain thermal inversions in the upper atmospheres of irradiated giant planets? *Astrophys. J.* **699**, 1487–1500 (2009).
- Atreya, S. K. & Wong, A. S. Coupled clouds and chemistry of the giant planets—a case for multiprobes. *Space Sci. Rev.* **116**, 121–136 (2005).
- Owen, T. *et al.* A low-temperature origin for the planetesimals that formed Jupiter. *Nature* **402**, 269–270 (1999).
- Seager, S. *et al.* On the dayside thermal emission of hot Jupiters. *Astrophys. J.* **632**, 1122–1131 (2005).
- Yung, Y. & DeMore, W. B. *Photochemistry of Planetary Atmospheres* (Oxford University Press, 1999).
- Hubeny, I., Burrows, A., & Sudarsky, D. A possible bifurcation in atmospheres of strongly irradiated stars and planets. *Astrophys. J.* **594**, 1011–1018 (2003).
- Fossati, L. *et al.* A detailed spectrophotometric analysis of the planet-hosting star WASP-12. *Astrophys. J.* **720**, 872–886 (2010).
- Pollack, J. B. *et al.* Formation of the giant planets by concurrent accretion of solids and gas. *Icarus* **124**, 62–85 (1996).
- Lodders, K. Jupiter formed with more tar than ice. *Astrophys. J.* **611**, 587–597 (2004).



26. Fortney, J. J., Marley, M. S., & Barnes, J. W. Planetary radii across five orders of magnitude in mass and stellar insolation: application to transits. *Astrophys. J.* **659**, 1661–1672 (2007).
27. Line, M. R., Liang, M. C. & Yung, Y. L. High-temperature photochemistry in the atmosphere of HD 189733b. *Astrophys. J.* **717**, 496–502 (2010).
28. Cushing, M. C., Rayner, J. T. & Vacca, W. D. An infrared spectroscopic sequence of M, L, and T dwarfs. *Astrophys. J.* **623**, 1115–1140 (2005).
29. Castelli, F. & Kurucz, R. L. New grids of ATLAS9 model atmospheres. Preprint at (<http://arxiv.org/abs/astro-ph/0405087>) (2004).
30. Lopez-Morales, M. *et al.* Day-side z'-band emission and eccentricity of WASP-12b. *Astrophys. J.* **716**, L36–L40 (2010).

**Supplementary Information** is linked to the online version of the paper at [www.nature.com/nature](http://www.nature.com/nature).

**Acknowledgements** We thank the authors of ref. 5 for sharing their ground-based observations before publication, and Thomas J. Loredo for discussions. N.M. thanks

S. Seager for financial support during his stay at MIT, where most of the modelling work was carried out. This work is based on observations made with the Spitzer Space Telescope, which is operated by the Jet Propulsion Laboratory, California Institute of Technology, under a contract with NASA. Support for this work was provided by NASA through an award issued by JPL/Caltech.

**Author Contributions** N.M. conducted the atmospheric modelling and wrote the paper with input on both from J.H.; J.H. and P.J.W. led the observing proposals, data from which have been interpreted in this work; J.H., J.B. and C.J.C. designed the observations with input from P.J.W., D.R.A., A.C.-C., L.H., C.H., P.F.L.M., D.P. and R.G.W.; J.H., K.B.S., S.N., C.J.C., D.D., J.B., R.A.H., N.B.L., D.R.A., A.C.-C., C.B.T.B. and W.C.B. analysed the Spitzer data.

**Author Information** Reprints and permissions information is available at [www.nature.com/reprints](http://www.nature.com/reprints). The authors declare no competing financial interests. Readers are welcome to comment on the online version of this article at [www.nature.com/nature](http://www.nature.com/nature). Correspondence and requests for materials should be addressed to N.M. ([nmadhu@mit.edu](mailto:nmadhu@mit.edu)).